Azimuth High Resolution for a Conically Scanned Pencil-Beam Scatterometer Using Rotating Azimuth Doppler Discrimination Postprint

Authors: Wang, Gang, Dong, Xiaolong, Zhu, Di, Bao, Qingliu

Date: 2017-03-10T00:00:00+00:00

Abstract

In order to satisfy a relatively high resolution for the retrieval of snow water equivalent, an X/Ku-band dual-frequency full-polarized SCATterometer (DFP-SCAT) onboard Water Cycle Observation Mission (WCOM) satellite is designed for high-resolution observations. However, given the following situations, the method called "rotating azimuth Doppler discrimination" is proposed, which can satisfy the resolution requirement and real-time processing: 1) the conically rotation rate of antenna is relatively fast; 2) the swath width is larger than 1000 km; and 3) day or night observation capabilities are required. Considering the complexity of the system' s design and the improvement of azimuth resolution capability, a burst pulsing scheme is addressed to satisfy the numbers of azimuth sampling. The simulation model is used to analyze the feasibility of azimuth discrimination method based on geometry and system parameters. It is shown that the achievable azimuth resolution is about 2–5 km at far end of the swath and only 5km at near end of the swath. The results show that when the size of a slice is set as 2–5 km, the Kpc is about less than 0.4 as snow depth varies, and the Kpc of combined slices is smaller than a single slice.

Full Text

Preamble

Azimuth High-Resolution for a Conically Scanned Pencil-beam Scatterometer Using Rotating Azimuth Doppler Discrimination

Gang Wang, Xiaolong Dong, Senior Member, IEEE, Di Zhu, Member, IEEE, and Qingliu Bao

Abstract—To satisfy the relatively high resolution requirements for snow water equivalent retrieval, an X/Ku-band dual-frequency fully polarimetric SCAT-

terometer (DFPSCAT) onboard the Water Cycle Observation Mission (WCOM) satellite is designed for high-resolution observations. However, given the constraints of i) a relatively fast conical rotation rate of the antenna (19 r/min), ii) a swath width larger than 1000 km, and iii) required day-and-night observation capabilities, a method called "Rotating Azimuth Doppler Discrimination" is proposed that can meet both the resolution requirements and real-time processing needs. Considering system design complexity and the improvement of azimuth resolution capability, a burst pulsing scheme is implemented to satisfy the required number of azimuth samples. A simulation model is used to analyze the feasibility of the azimuth discrimination method based on geometry and system parameters. Results show that an achievable azimuth resolution of approximately 2–5 km can be obtained at the far end of the swath, and only 5 km at the near end. The results demonstrate that Kpc is <0.4 when snow thickness exceeds 5 m and approximately 0.75 for light snow conditions.

Index Terms—Scatterometer, Rotating Antenna, Doppler Discrimination, burst pulse scheme

I. INTRODUCTION

The Water Cycle Observation Mission (WCOM) proposes a DFPSCAT utilizing dual frequencies (X-band at 9.6 GHz and Ku-band at 17 GHz) and multi-polarization for mapping snow water equivalent and freeze-thaw processes [1, 2], aiming to provide higher accuracy and consistent measurements of key water cycle elements from space, including soil moisture, ocean salinity, freeze-thaw state, and snow water equivalent. Spaceborne scatterometers have provided great benefit to numerical weather prediction and climate monitoring over the past 40 years, with various designs and developments applied to different applications. The measurement accuracy and performance for snow water equivalent retrieval are directly related to spatial resolution. To account for local vegetation variability, the resolution should be improved to a higher resolution of 1 km [3].

However, such high resolution is difficult to achieve with current scatterometer instruments, which have an inherent spatial resolution on the order of 10–50 km [4, 5]. Therefore, considering the implementation capabilities of DFPSCAT onboard WCOM, a spatial resolution of 2–5 km is proposed [2].

Unlike synthetic aperture radar (SAR), real aperture radar (RAR) provides measurements through real-time processing. However, especially when the antenna scans rapidly, the accumulation time of RAR is not long enough, resulting in relatively low resolution. In contrast to a fan-beam system, the pencil-beam design employs a single antenna that conically scans about the nadir axis to provide multiple azimuth measurements. Such a pencil-beam antenna is also easier to install on the spacecraft [6]. Based on the platform motion and antenna scanning style of the onboard scatterometer, this system achieves improved resolution along the azimuth direction using the Doppler discrimination method.

This method is applied when the azimuth angle is in the range between 10 to 170 degrees [7, 8]. When the azimuth is within the intervals of 0±10 and 180±10 degrees (where the absolute value of Doppler shift is largest and the Doppler bandwidth is near zero), a method called super-resolution reconstruction is applied [9]. However, this is not the focus of this paper. Therefore, a tradeoff between azimuth resolution and system complexity deserves careful consideration. Meanwhile, a compromise between high-accuracy measurement of the backscattering coefficient and relatively high resolution should be considered.

Section II introduces the system parameters and burst pulse scheme. In Section III, we analyze the azimuth signals and introduce the rotating azimuth Doppler discrimination method. Section IV presents simulations of point targets. Finally, summary and concluding remarks are given in Section V.

II. INSTRUMENT DESIGN OF THE SCANNING PENCIL-BEAM SCATTEROMETER

A. System Parameters

The DFPSCAT onboard WCOM will observe the Earth for 3 years from a sun-synchronous, near-circular orbit with an equator-crossing altitude near 600 km, operating at two frequencies with four polarizations (VV, HH, VH, HV) [10]. The spaceborne scanning pencil-beam scatterometer can provide high signal-to-noise ratio (SNR) and the advantage of covering a larger area than SAR. The DFPSCAT instrument is a dual-frequency polarimetric radar scatterometer consisting of a mechanically scanned radiometer with a 1.5 m diameter reflector antenna, which can satisfy the requirements of high SNR and high gain. Key specifications are shown in [TABLE:N].

The DFPSCAT instrument is based on a single reflector measuring up to 1.5×1.5 m, illuminated by two adjacently placed feeds that generate multiple beams. A single rotating antenna allows a larger swath of measurements at a constant incidence angle. To obtain a ground swath of about 1000 km, the antenna incidence angle must be at least 39°, as calculated using the observation geometry, see [FIGURE:1]. Considering the "along-track continuity constraint," the rotation rate should be given by the relationship between ground velocity, elevation footprint width, and antenna rotation rate. The rotation rate should be at least 19 revolutions per minute (RPM) to achieve complete surface coverage over the swath.

The antenna scanning loss is defined by the beam patterns on the surface at the times of transmit and receive. The integral range covers the entire footprint. The scanning loss of a reflector antenna is represented as a function of the beam patterns on the surface at the times of transmit and receive, see [FIGURE:2]. The speed of the footprint due to satellite motion in the azimuth direction is far smaller than the speed caused by scanning motion, so scanning loss is an important consideration. Given the rapid scanning motion of the antenna,

analysis based on the radar ambiguity function is particularly useful for the pencil-beam scatterometer. Here, the scanning loss is a function of azimuth displacement normalized by the two-way azimuth beamwidth. Because the same antenna is used for transmit and receive, the scanning loss should be carefully calculated. When the antenna rotates at 19 RPM, the antenna scanning loss is approximately -1.3 dB.

B. Radar Pulse Repetition Frequency

The azimuth resolution in traditional scatterometers is equal to the azimuth footprint, which is very coarse. To unambiguously resolve the scene in azimuth, the PRF should be at least larger than the total Doppler bandwidth across the azimuth footprint. For Ku-band, the azimuth footprint corresponds to a Doppler bandwidth of approximately 10 kHz, thus requiring a minimum PRF of 10 kHz. Meanwhile, to avoid range ambiguities within the footprint, a maximum PRF of 9.46 kHz is required, corresponding to a beam fill time of about 0.106 ms. The resolution is only improved in one dimension for traditional pulse design, so a tradeoff between range ambiguities and azimuth ambiguities should be considered [11]. One way to resolve this problem is to use a burst pulsing scheme [6].

In [FIGURE:3], the echo returns are depicted as semicircles, where `intTbTrecTbTintT` represents the time interval of pulses in a transmit burst, the length of the transmit burst, and the length of the receive burst. A multiple-pulse burst of length is repeated at the burst repetition interval (BRI).

The DFPSCAT radar emits H-polarized and V-polarized pulse pairs at a burst repetition interval of approximately 250 Hz, which is 1.2 ms, and is 75 microseconds, which is modulated to a linear frequency modulation (LFM) chirp of 2 MHz bandwidth. In a transmit burst, the radar emits 16 H-polarized and 16 V-polarized pulses. For the transmit burst, pulses adopt different carrier frequencies for adjacent pulses. In the process of echo returns reception, pulses are distinguished by de-chirp method, see [FIGURE:4]. In a receive window, there will be several pulses with different carrier frequencies. In the simulation process, the voltage of H polarization is double that of V polarization. Although these pulses overlap in the time domain, the pulses can be separated by using a receive window corresponding to different carrier frequencies [12]. In FIGURE:4, there are five pulses in a receive window. The desired signal is what we want in this receive window. In FIGURE:4, the pulses are processed using a simple lowpass filter, and such processing cannot compensate for phase variation or frequency shift [13].

III. THE AZIMUTH RESOLUTION

The scatterometer antenna not only flies at a speed of about 7550 m/s but also rotates about the nadir axis at a stable rate. The roundtrip flight time for the beam pulse is approximately 5.26 ms, which can cause a relatively large rotation

angle of the antenna (about 0.6°). The effective area illuminated by the antenna is defined by the 3 dB bandwidth. If the dimension of an antenna is designed large enough, the azimuth resolution can achieve several kilometers, but a large antenna brings great difficulties for onboard implementation. To achieve global seamless coverage, this paper employs a pencil-beam antenna at a rate of 19 RPM based on the along-track continuity constraint, as mentioned earlier.

A. The Analysis of Azimuth Resolution

Based on the burst pulsing scheme design, the PRF can reach about ten kHz. As previously discussed, PRF should be higher than the Doppler bandwidth of the -3 dB footprint. Errors caused by satellite motion and orientation will lead to errors in Doppler centroid real-time estimation. However, this system has high-precision orbit information. The performance requirement for attitude control error reaches 0.05 degrees, and in practice the attitude control error can reach 0.01 degrees.

When the antenna is perpendicular to the flight direction (azimuth = 90° or 270°), the system achieves maximum Doppler bandwidth, and the iso-delay and iso-Doppler contours are locally perpendicular to the elevation and azimuth axes respectively. When the antenna scans to the forward or aft looking directions (azimuth = 0° or 180°), the iso-Doppler lines are parallel to the azimuth axis. In this case, the Doppler bandwidth of the azimuth footprint is almost zero. Thus it is difficult to achieve high azimuth resolution when the antenna scans to the forward or aft looking directions. From FIGURE:5, the cross-track distance (CTD) is defined as the vertical distance between a given measurement and the nadir track.

As the antenna rotates, the achievable azimuth resolution is defined as:

$$\delta_{az} = \frac{\lambda R_0}{2V_{sat}T_{dw}} \cdot f_{az}(\theta)$$

where $f_{az}(\theta)$ represents the degradation in azimuth resolution due to squint elongation effects, θ is the azimuth angle, λ is the wavelength, R_0 is the slant range, V_{sat} is the satellite speed, and T_{dw} is the effective dwell time, which is approximately one half of T_b. The dwell time is inversely proportional to Doppler resolution. The burst pulsing scheme comes at the price of a factor of two or three decrease in achievable azimuth resolution compared with traditional pulse design.

From FIGURE:5, when the CTD is in the range of 200 to 500 km, the azimuth resolution can reach 2 km, and when the CTD is about 80 km, the azimuth resolution can only reach 5 km. When the CTD is less than 80 km, other methods are used, which are not the focus of this paper [9].

B. A Rotating Azimuth Doppler Discrimination

The conically scanned pencil-beam antenna rotates as it moves along the flight direction. Meanwhile, the system must meet requirements for real-time processing and long-term data storage. Therefore, the processing algorithm must be simple and efficient, suitable for actual use on the satellite. The processing algorithm called "Rotating Azimuth Doppler Discrimination" can meet these design requirements.

From the observation geometry, the echoes returned from a footprint can be written as:

$$s(t,\tau) = \iint_{footprint} \sigma(r,x) \cdot rect\left(\frac{\tau - 2R(t,r,x)/c}{T_p}\right) \cdot \exp\left(-j\frac{4\pi f_0}{c} R(t,r,x)\right) \cdot \exp\left(j\pi\gamma\left(\tau - \frac{2R(t,r,x)}{c}\right)^2\right) dr$$

where $rect(\cdot)$ is a rectangular window, $\sigma(r,x)$ is the backscattering coefficient of target (r,x), f_0 is the transmit carrier frequency, T_p is the width of the transmit pulse, γ is the frequency modulation rate, c is the speed of light, τ and t are range and azimuth time (called "fast" time and "slow" time), and $R(t,r,x)$ is the distance between the target and the transmitter.

From FIGURE:6, the relations between slow-time and frequency domain Doppler are described [14]. B_d is the target Doppler bandwidth, T_d is the dwell time of the target, a_k is the Doppler rate, and $\dot{f}_{rot}$ is the Doppler centroid varying rate, which is given as follows:

$$\dot{f}_{rot} = \frac{\partial f_{dc}}{\partial t} = \frac{2V_{sat}\sin\theta_{rot}\sin\theta_{inc}}{\lambda}$$

where θ_{rot} is the angular velocity and θ_{inc} is the antenna incidence angle. From FIGURE:6 and FIGURE:6, B_d is maximum at targets S1 and S7, and minimum at target S4. As the antenna scans forward or backward, the Doppler bandwidth and Doppler centroid change nonlinearly.

The block diagram of the model is shown in [FIGURE:7] [15]. The first step is to remove the carrier frequency from raw data, then the next step is to adopt the de-chirp method by introducing an azimuth product between the signal and the following chirp signal:

$$H = \exp\left(-j2\pi f_d \tau\right) \cdot \exp\left(j\pi\gamma\tau^2\right)$$

where f_d is the carrier frequency and R_d is the reference slant range, with $\tau_d = 2R_d/c$. The next three steps remove the residual video phase using range FFT and range inverse FFT, where H_2 is given as follows:

$$H_2 = \exp\left(j\pi \frac{f_r^2}{\gamma}\right)$$

where f_r is the frequency sampling in the range direction.

IV. SIMULATION EXPERIMENT

A. Point Target Response Analysis

The simulation parameters are described in [TABLE:N]. A group of transmit bursts is used, producing a PRF of about 13.3 kHz. The model is used to analyze point targets first for the side-looking case, then extended to the case of an arbitrary azimuth angle. The spacecraft nadir on the surface is defined as the coordinate origin. The flight direction is defined as the X axis and the cross-track direction as the Y axis. When the azimuth angle is 90°, two targets 5 km apart have coordinates (-2.5e3, 500e3, 0) and (2.5e3, 500e3, 0), and two targets 2 km apart have coordinates (-1e3, 500e3, 0) and (1e3, 500e3, 0), given in units of meters.

From [FIGURE:8], targets that are 2 km apart can be distinguished using the model when the azimuth is in the range of 60 to 90 degrees, which is consistent with previous analysis. However, when the azimuth is 30°, targets that are 2 km apart cannot be separated because the Doppler resolution is slightly larger than the Doppler bandwidth between them. At the same azimuth scope, the larger the distance between targets, the better the separation capability. The transmit burst time is 1.2 ms, corresponding to a scanning distance of 1.2 km. Thus the total coverage distance along the rotating direction in one burst time is about 15 km. When the azimuth is 30°, if the azimuth resolution is 5 km, then the scanning distance should be at least 10 km.

Because the azimuth resolution quickly degrades near the nadir track due to elongation effects, when the azimuth is in the range of 10 to 30°, the azimuth resolution should be set to about 5 km. Therefore, the azimuth resolution can reach 2 km at the far end of the swath and 5 km at the near end.

B. Communication Error Kpc

The calculation of Kpc for a pencil-beam rotating scatterometer may be quite complex, especially for combined slices [16]. The detected energy from several slices is summed, and a composite calibration factor is applied [17]. The normalized standard deviation of the estimate can be expressed as:

$$K_{pc} = \sigma_0 \sqrt{\frac{1}{N_{el}N_{az}}\left(1+\frac{1}{SNR}\right)^2 + \frac{1}{SNR^2}}$$

where SNR is the signal-to-noise ratio, N_{el} is the number of independent looks in elevation, and N_{az} is the equivalent number of azimuth looks.

The simulation data is based on the dense media radiative transfer (DMRT) model [18]. We choose the spatial resolution of a snow vector cell as 5 km × 5 km and assume that energy estimates are uncorrelated from slice to adjacent slice. From

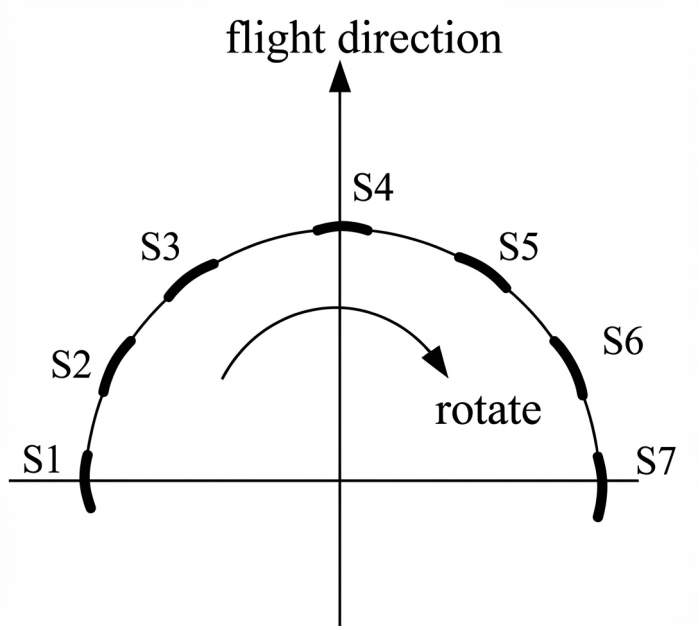

Figure 1: Figure 9

(a) and

(b), Kpc will reduce with snow accumulation because of higher SNR. When snow thickness exceeds 5 m, the Kpc of different combined slices can reach 0.4. However, Kpc is relatively large for shallow snow because SNR is low. Kpc depends on the combination of slice number, slice size, and SNR. From

(b), the Kpc of 3 km and 5 km combined slices is relatively small compared with 4 km combined slices.

V. CONCLUSION

In this paper, a "Rotating Azimuth Doppler Discrimination" method is introduced and analyzed, which can achieve azimuth resolution of 2-5 km at the far end of the swath and only 5 km at the near end. Various options considered for improving azimuth resolution are compared. A key design of the burst pulse scheme is proposed that can reach 13.3 kHz PRF. Because the scatterometer

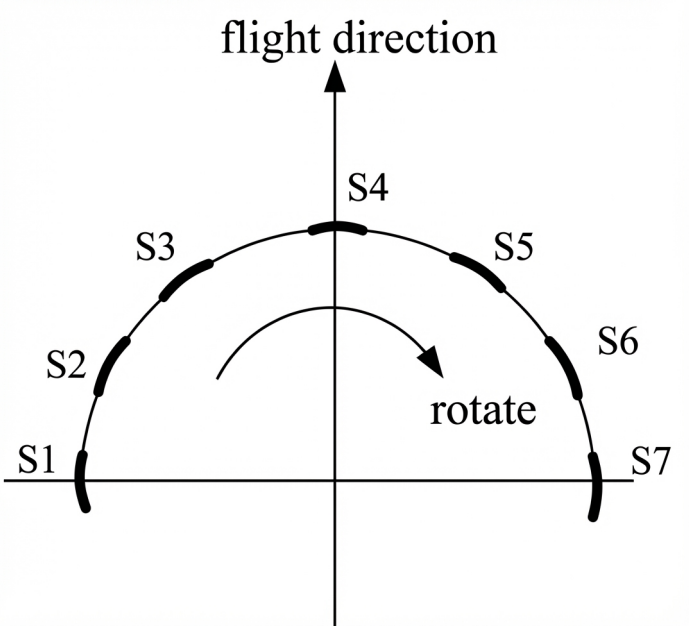

Figure 2: Figure 9

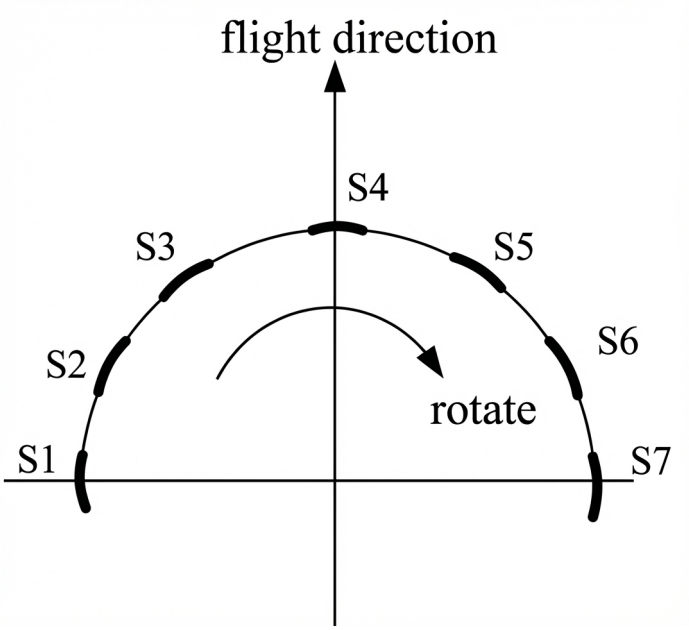

Figure 3: Figure 9

obtains a large swath of 1000 km in real-time and operates day or night, a rotating azimuth Doppler discrimination technique is employed to improve resolution simply and efficiently. Although azimuth resolution can reach a high level of 2–5 km at the near end of the swath, the normalized standard deviation of the estimate is relatively high, which may exceed 0.5. A series of simulations for point targets have been presented to verify the feasibility and validity of this method. Results show that the scatterometer can obtain high azimuth resolution using the "Rotating Azimuth Doppler Discrimination" method. In the future, simulations and experiments using different parameters will be carried out.

REFERENCES

[1] J. Shi, X. Dong, T. Zhao, J. Du, L. Jiang, Y. Du, H. Liu, Z. Wang, D. Ji, and C. Xiong, "WCOM: The science scenario and objectives of a global water cycle observation mission," in Proc. IEEE IGARSS Conf., Québec, QC, Canada, Jul. 12-18, 2014, pp.3646-3649.

[2] X. Dong, H. Liu, Z. Wang, J. Shi and T. Zhao, "WCOM: The mission concept and payloads of a global water cycle observation mission,"in Proc. IEEE IGARSS Conf., Québec, QC, Canada, Jul. 12-18, 2014, pp.3338-3341.

[3] G. Macelloni, M. Brogioni, F. Montomoli, G. Fontanelli, M. Kern, and H. Rott, "Evaluation of vegetation effect on the retrieval of snow parameters from backscattering measurements: A contribution to CoReH2O mission," in Proc. IEEE IGARSS Conf., Honolulu, HI, Jul. 25-30, 2010, pp.1772-1775.

[4] M.W. Spencer, Wu Chialin, and D.G. Long, "Improved resolution backscatter measurements with the SeaWinds pencil-beam scatterometer," in IEEE Trans. Geosci. Remote Sens., vol.38, no.1, pp.89-104, Jan. 2000.

[5] M.W. Spencer, Wu Chialin, and D.G. Long, "Tradeoffs in the design of a spaceborne scanning pencil beam scatterometer: application to SeaWinds," in IEEE Trans. Geosci. Remote Sens., vol.35, no.1, pp.115-126, Jan. 1997.

[6] M. W. Spencer, "A methodology for the design of spaceborne pencil-beam scatterometer systems," Ph.D. dissertation, Department of Electrical and Computer Engineering, Brigham Young University, 2001.

[7] M.W. Spencer, Tsai Wu-Yang, and D.G. Long, "High-resolution measurements with a spaceborne pencil-beam scatterometer using combined range/Doppler discrimination techniques," in IEEE Trans. Geos. Remote Sens., vol.41, no.3, pp.567-581, Mar. 2003.

[8] M.W. Spencer, Tsai Wu-Yang, and D.G. Long, "High resolution scatterometry by simultaneous range/Doppler discrimination," in Proc. IEEE IGARSS Conf., Honolulu, HI, 2000, pp.3166-3168.

[9] B.A. Williams and D.G. Long, "Reconstruction from aperture-filtered samples with application to scatterometer image reconstruction," in IEEE Trans.

Geosci. Remote Sens., vol.49, no.5, pp.1663-1676, May. 2011.

[10] J. Shi, "Snow water equivalence retrieval using X and Ku band dual-polarization radar," in Proc. IGARSS, Denver, CO, 2006, pp.2183-2185.

[11] F. T. Ulaby, R. K. Moore, and A. K. Fung, Microwave Remote Sensing Active and Passive, vol. 2, 1982, Addison-Wesley House.

[12] Q. Bao, X. Dong, D. Zhu, S. Lang, and X. Xu, "The feasibility of ocean surface current measurement using pencil-beam rotating scatterometer,"in IEEE Journal of Selected Topics in Applied Earth Observations and Remote Sensing, vol.8, no.7, pp.3441-3451, Jul. 2015.

[13] W. Xu, P. Huang, Y. Deng, J. Sun, and X. Shang, "An efficient approach with scaling factors for TOPS-Mode SAR data focusing," in IEEE Geosci. Remote Sens. Lett., vol.8, no.5, pp.929-933, Oct. 2011.

[14] A. Moreira, R. Scheiber, and J. Mittermayer, "Azimuth and range scaling for SAR and ScanSAR processing," in Proc. IEEE Int. Geosci. Remote Sens., Symp., Lincoln, NE, USA, 1996, pp. 1214–1216.

[15] D.G. Long and M.W. Spencer, "Radar backscatter measurement accuracy for a spaceborne pencil-beam wind scatterometer with transmit modulation," in IEEE Trans. Geosci. Remote Sens., vol.35, no.1, pp.102-114, Jan. 1997.

[16] X. Dong, S. Lang, T. Wang, and H. Liu, "Accuracy and resolution analysis of the pencil beam radar scatterometer onboard China' s HY-2 satellite," in IEEE Geosci. Remote Sens. Symp., 2007, pp. 4467-4470.

[17] L. Tsang, J. Pan, D. Liang, Z. Li, D.W. Cline, and Y. Tan, "Modeling active microwave remote sensing of snow using dense media radiative transfer (DMRT) theory with multiple-scattering effects," in IEEE Trans. Geosci. Remote Sens., vol.45, no.4, pp.990-1004, Apr. 2007.